GROWTH FACTORS, CYTOKINES, AND CELL CYCLE MOLECULES

Rap1 GTPase Inhibits Tumor Necrosis Factor-α—Induced Choroidal Endothelial Migration via NADPH Oxidase— and NF-κB—Dependent Activation of Rac1

Haibo Wang,* Lori Fotheringham,* Erika S. Wittchen,[†] and M. Elizabeth Hartnett*

From The John A. Moran Eye Center,* University of Utah, Salt Lake City, Utah; and the Department of Cell Biology and Physiology,[†] University of North Carolina at Chapel Hill, Chapel Hill, North Carolina

Macrophage-derived tumor necrosis factor (TNF)-α has been found in choroidal neovascularization (CNV) surgically removed from patients with age-related macular degeneration. However, the role of TNF-α in CNV development remains unclear. In a murine laser-induced CNV model, compared with un-lasered controls, TNF-α mRNA was increased in retinal pigment epithelial and choroidal tissue, and TNF-α colocalized with lectin-stained migrating choroidal endothelial cells (CECs). Inhibition of TNF-α with a neutralizing antibody reduced CNV volume and reactive oxygen species (ROS) level around CNV. In CECs, pretreatment with the antioxidant apocynin or knockdown of p22phox, a subunit of NADPH oxidase, inhibited TNF-α—induced ROS generation. Apocynin reduced TNF-α—induced NF-κB and Rac1 activation, and inhibited TNF-α—induced CEC migration. TNF-α—induced Rac1 activation and CEC migration were inhibited by NF-κB inhibitor Bay11-7082. Overexpression of Rap1a prevented TNF-α—induced ROS generation and reduced NF-κB and Rac1 activation. Activation of Rap1 by 8-(4-chlorophenylthio) adenosine-2′-O-Me-cAMP prevented TNF-α—induced CEC migration and reduced laser-induced CNV volume, ROS generation, and activation of NF-κB and Rac1. These findings provide evidence that active Rap1a inhibits TNF-α—induced CEC migration by inhibiting NADPH oxidase-dependent NF-κB and Rac1 activation and suggests that Rap1a de-escalates CNV development by interfering with ROS-dependent signaling in several steps of the pathogenic process. *(Am J Pathol 2015, 185: 3316—3325; http://dx.doi.org/10.1016/j.ajpath.2015.08.017)*

Neovascular age-related macular degeneration (AMD) is the leading cause of legal blindness in people >60 years.[1] Intravitreal injection of anti—vascular endothelial growth factor (VEGF) agents has become the standard of care for choroidal neovascularization (CNV) in neovascular AMD; however, reports indicate approximately 40% of patients with neovascular AMD respond to anti-VEGF treatment.[2] One reason may be that treatment is provided too late when CNV is already present. To address this possibility, we focus on understanding early steps in the pathophysiology in neovascular AMD to prevent vision loss. Activation and migration of choroidal endothelial cells (CECs) are early steps in the development of CNV. Activated CECs migrate through the Bruch membrane toward the retinal

pigment epithelium (RPE) and also transmigrate the RPE into the sensory retina. At either location, activated CECs can proliferate to form CNV. Severe vision loss occurs when CNV develops in the sensory retina.[3,4]

Both inflammation and oxidative stress have been implicated in the development of CNV.[5] The inflammatory

cytokine, tumor necrosis factor (TNF)-α, was found in macrophages within CNV surgically removed from patients with neovascular AMD.[6] Inhibition of TNF-α bioactivity by neutralizing antibodies[7] or by targeting TNF-α receptor 1[8] reduced the volume and leakage of laser-induced CNV in experimental models, suggesting that TNF-α−mediated signaling was important in the development of CNV.[9,10] The roles of TNF-α−mediated inflammation in rheumatoid arthritis, Alzheimer disease, atherosclerosis, and diabetes have been well established,[11] and activation of NF-κB by TNF-α plays a fundamental role in these chronic inflammatory diseases.[12] Recent studies also provide evidence to support the role of TNF-α in the regulation of oxidative stress. In microglia cells, TNF-α induced mitochondrial reactive oxygen species (ROS) generation.[13] In coronary microvascular endothelial cells (ECs), TNF-α−induced ROS generation was blocked in cells depleted of $p47^{phox-/-}$, a subunit of NADPH oxidase,[14] suggesting that NADPH oxidase was involved in the TNF-α−mediated ROS generation. Additional evidence in dermal microvascular ECs indicated that activation of NF-κB, a downstream effector of TNF-α−mediated inflammatory signaling, was involved in TNF-α−induced ROS generation and involved NADPH oxidase activation.[15] In aortic vascular ECs, cross talk between oxidative and inflammatory pathways was proposed to affect endothelial dysfunction and cardiovascular disease.[16]

We previously found that VEGF promoted CEC migration by activating the small GTPase Rac1.[17,18] Inhibition of Rac1 activity through molecular or pharmacological approaches prevented VEGF-induced CEC migration and also reduced ROS generated by NADPH oxidase.[19] We then found that activation of another GTPase protein, Rap1, increased RPE barrier integrity and reduced CNV volume in a murine laser injury model by inhibiting NADPH oxidase−dependent ROS generation in RPE.[20,21] Herein, we study another pathway that involves ROS generation through the inflammatory cytokine TNF-α, specifically testing the hypothesis that TNF-α induces CEC migration via NADPH oxidase−generated ROS, in which activation of Rac1 is downstream of ROS, and that activation of Rap1 prevents TNF-α−induced CEC migration by reducing ROS generation. On the basis of previous studies in other tissues, we postulate that interactions between inflammatory and oxidative signaling mechanisms overwhelm homeostatic mechanisms in the outer retina, which would normally prevent the formation of CNV. Through at least two interconnected signaling pathways that augment CEC migration, CNV can develop, such as that in neovascular AMD.

Materials and Methods

Animals

C57/BL/6 wild-type female mice, aged 5 to 8 weeks, were used (Charles River, San Diego, CA). All animal procedures were conducted in accordance with the University of Utah (Salt Lake City, UT) for the Guide for the Care and Use of Laboratory Animals[22] and the Association for Research in Vision and Ophthalmology Statement for the Use of Animals in Ophthalmic and Vision Research.

Laser-Induced CNV Model and Injections

The laser-induced CNV model was used as previously described.[19] The i.p. injections of 100 mg/kg ketamine (Hospira, Inc., Lake Forest, IL) and 20 mg/kg xylazine (AnaSed Lloyd Laboratories, Shenandoah, IA) were used for anesthesia. After mydriasis with 1% tropicamide ophthalmic solution (Bausch & Lomb, Rochester, NY), mice were raised onto a platform, and a coupling agent, GenTeal (Alcon, Fort Worth, TX), was applied to the cornea (Novartis, East Hanover, NJ). Laser photocoagulation was performed (532-nm diode laser, 400-mW intensity, 100-millisecond duration; Iridex, Mountain View, CA) using the laser module of the Phoenix Micron IV Imaging System (Phoenix Research Labs, Pleasanton, CA). Five to six laser spots per eye were applied approximately two disk diameters from the optic nerve, avoiding major vessels. Disruption of the Bruch membrane was confirmed by the appearance of a cavitation bubble. Right after laser injury, using a Microliter syringe (Hamilton Company, Reno, NV), an i.v. injection of total volume of 1 μL of 20.5 μmol/L 8-(4-chlorophenylthio) adenosine-2-O-Me-cAMP (8CPT; Calbiochem, La Jolla, CA)[20] and/or 50 ng/mL neutralizing anti-mouse TNF-α antibody (Ab; R&D Systems, Minneapolis, MN) and 50 ng/mL control isotype IgG (R&D Systems) or phosphate-buffered saline (PBS). The i.v. 8CPT injections can access CNV and increase Rap1 activity in RPE/choroids.[20] Groups with different injections were 0.5 μL PBS + 0.5 μL IgG, 0.5 μL 8CPT + 0.5 μL IgG, 0.5 μL TNF-α Ab + 0.5 μL PBS, and 0.5 μL TNF-α Ab + 0.5 μL 8CPT. Both eyes of each mouse were lasered and injected with the same reagent. Five days after laser, mice were euthanized and one eye from each mouse was collected for RPE and choroidal flat mount analysis and the fellow eye for dihydroethidium (DHE; Invitrogen, Carlsbad, CA) fluorescence staining of RPE/choroids or for protein analyses by immunostaining of chorioretinal sections or Western blot analysis. Each group included both eyes of eight mice.

Analysis of Lesion Volume in RPE/Choroidal Flat Mounts

Eyes were first fixed in 4% paraformaldehyde (Electron Microscopy Sciences, Hatfield, PA) for 1 hour. After removal of cornea, lens, retina, and vitreous, posterior eyecups of the RPE, choroid, and sclera were dissected. Eyecups were stained with AlexaFluor 568−conjugated isolectin B4 (Invitrogen) overnight at 4°C to label invading choroidal vessels. The eyecups were then flattened by cutting radial incisions and flat mounted onto a microscope slide with Fluoromount G (Southern Biotech, Birmingham,

AL) for confocal imaging. Flat mounts were imaged by taking optical Z-sections at 5-µm increments with a confocal microscope (FV1000; Olympus, Tokyo, Japan). Each CNV lesion volume (µm^3) was measured by computerized image analysis using Fluoview software version 4.1 provided with the microscope. Lesions with obvious hemorrhage or bridging CNV were excluded. Each CNV spot was considered an independent data point. For each condition, at least 25 spots were analyzed from eight different mice.

ROS Generation Assay in RPE/Choroidal Sections Surrounding CNV Lesions by DHE Staining

ROS generation in RPE/choroids was detected by measuring DHE fluorescence, as previously described.[19] Briefly, fresh-frozen sections of RPE-choroids were thawed, washed in Tris-buffered saline, and incubated with 10 µmol/L DHE in the dark at 37°C for 15 minutes. Slides were rinsed and mounted with DAPI Fluoromount-G (SouthernBiotech, Birmingham, AL) mounting medium. Images were acquired with a confocal microscope (Olympus). The area of the lesion and neovascular tissue in laser-burned sections and the integrated density of DHE staining per image area of interest were measured using ImageJ version 1.43 (NIH, Bethesda, MD; http://imagej.nih.gov/ij). The integrated densities of sections of CNV from several mice were analyzed for each condition. For each condition, at least 10 spots were analyzed from four different mice.

Preparation and Immunostaining of Retinal and RPE/Choroidal Sections

Eyes were first fixed in 4% paraformaldehyde for 1 hour, and then corneas and lenses were removed. Eye cups were incubated in 30% sucrose overnight and frozen at −80°C after immersion in OCT compound (Tissue Tek; EMS, Hatfield, PA). Eye cups were cut into cryosections (12 µm thick). Sections were incubated with either mouse anti−GTP-Rac1 (1:100; NewEast Biosciences, King of Prussia, PA) or anti−p-p65 (1:100; Cell Signaling Technology, Danvers, MA) overnight at 4°C. After rinsing, sections were incubated for 1 hour with fluorescein isothiocyanate−conjugated goat anti-mouse secondary Ab (1:100; Jackson ImmunoResearch Laboratories, Inc., West Grove, PA) and Alexa 568−conjugated Ab for isolectin B4 (lectin, 1:500; Invitrogen) to stain vessels. Sections stained with isotype IgG were used as controls. Labeling for all sections was performed during the same experimental session. Images were captured using confocal microscopy (model IX81; Olympus) at ×20 magnification.

Cell Culture

Human CECs were isolated from different donor eyes obtained from Utah Zions Eye Bank (Salt Lake City, UT), as described previously.[18] CECs were grown in endothelial growth medium (Lonza, Walkersville, MD) plus 5% fetal bovine serum, and cells from passages 2 to 5 were used for experiments.

Adenoviral Transduction and siRNA Transfection of CECs

CECs were transduced with adenoviral constructs expressing green fluorescent protein (Ad-GFP) or GFP-tagged active Rap1a (Ad-63E), kind gifts from Dr. Keith Burridge (University of North Carolina, Chapel Hill, NC), or transfected using Lipofectamine 2000 per commercial protocol (Life Technologies, Grand Island, NY) with siRNA targeting the human CYBA gene, Rac1 gene, or silencer-selective negative control siRNA (all from Life Technologies, Grand Island, NY). Forty-eight hours after viral transduction or transfection, cells were incubated with 20 ng/mL human recombinant TNF-α (R&D Systems) or PBS for 30 minutes for further analyses.

ROS Generation Assay in Cultured CECs

Intracellular ROS generation was measured as described previously.[21] CECs were loaded with 5-µm 2′,7′-dichloro-fluorescein (DCF; Invitrogen) in serum-free medium for 30 minutes at 37°C. After two washes with PBS, cells were pretreated with 100 µmol/L apocynin (Sigma-Aldrich, St. Louis, MO) or PBS for 30 minutes, then incubated with 20 ng/mL TNF-α or PBS for another 30 minutes. ROS generation was measured in a fluorescent plate reader at an excitation of 488 nm and an emission of 520 nm. Cells incubated with 10 µmol/L H_2O_2 were used as a positive control. For each condition, at least nine samples from three independent experiments were analyzed.

Pull-Down Assay of Rac1 Activation

CECs were pretreated with 100 µmol/L apocynin, 1 µmol/L Bay 11-7082 (Sigma-Aldrich), or dimethyl sulfoxide/PBS control for 30 minutes, then incubated with 20 ng/mL TNF-α or PBS for another 15 or 60 minutes. Cells were harvested for the Rac1 activity assay, as described previously.[18] Briefly, cell lysates were adjusted to equal protein concentration and volumes, and then incubated for 30 minutes at 4°C with 30 µg of glutathione S-transferase−(Rac1-binding domain of p21 activated kinase 1) fusion protein (kind gifts from Dr. Keith Burridge) immobilized on glutathione beads to specifically pull down active (GTP-bound) Rac1. The amount of active Rac1 versus total Rac1 was then determined by Western blot analysis with a monoclonal anti-Rac1 Ab (BD Biosciences, San Jose, CA), followed by a horseradish peroxidase−conjugated secondary anti-mouse Ab (Bio Rad, Hercules, CA). For each condition, at least six samples from two or three independent experiments were analyzed.

CEC Migration Assay

Transwell CEC migration assays were performed, as described previously.[23] Growth factor−reduced Matrigel
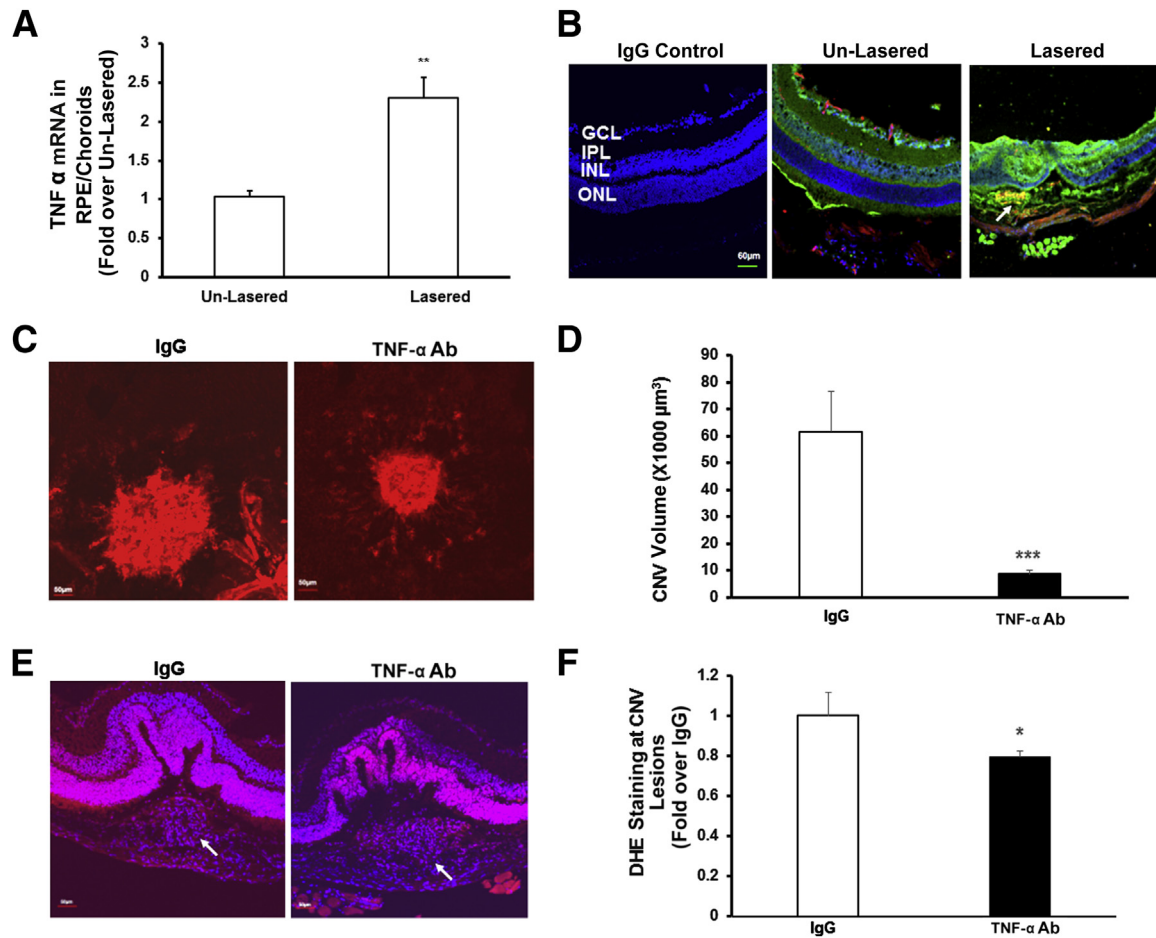
Figure 1 Tumor necrosis factor (TNF)-α mediates choroidal neovascularization and generation of reactive oxygen species around choroidal neovascularization (CNV) in the mouse laser-induced CNV model. **A** and **B:** Real-time PCR of mouse TNF-α mRNA in retinal pigment epithelium (RPE)/choroids (**A**) and immunostaining of TNF-α in retinochoroidal cryosections of C57Bl/6 6-week-old mice without laser treatment (un-lasered) or 5 days after laser (Lasered) (**B**). Red, lectin; blue, DAPI; green, TNF-α; and yellow, lectin + TNF-α. The **arrow** points to the area of CNV lesion colabeled with TNF-α and lectin. **C–F:** CNV volume (**C** and **D**) and dihydroethidium (DHE) staining in RPE/choroids surrounding CNV lesions (**E** and **F**) of mice injected with 50 ng isotype IgG (IgG) or 50 ng neutralizing TNF-α antibody (Ab). Representative images of CNV lesions (**C**) and DHE staining (**E**); quantification of CNV volume (**D**) and integrated density of DHE staining (**F**). Red, DHE; blue, DAPI; and purple, DHE + DAPI. The **arrow** points to the area of CNV lesion. $*P < 0.05$, $**P < 0.01$, and $***P < 0.001$. $n = 6$ (**A**); $n = 20$ (**D**). GCL, ganglion cell layer; INL, inner nuclear layer; IPL, inner plexiform layer; ONL, outer nuclear layer.

(100 μL) with 20 ng/mL human recombinant TNF-α was plated into each well of a 24-well plate. Two hours later, 500 μL of EBM-2 was added to each well, and a 6.5-mm-diameter Transwell insert (8-μm pores; Corning Incorporated, Corning, NY) was placed into the well. Human CECs in EBM-2 were prestained with Vybrant DiO cell-labeling solution (Invitrogen) for 30 minutes at 37°C and seeded into the Transwell inserts at 20,000 cells per 200 μL of EBM-2 media. The plates were incubated for 16 hours at 37°C, 5% CO_2, and migrated stained CECs were quantified using fluorescent microscopy. For each condition, at least six samples were analyzed.

Western Blot Analysis

CECs were lysed in radioimmunoprecipitation assay buffer (RIPA) with protease inhibitor cocktail (Roche Diagnostics, Indianapolis, IN) and orthovanadate (Sigma-Aldrich). Lysates were centrifuged at $16,000 \times g$ for 5 minutes at 4°C,

and the supernatants were collected. The total protein for each sample (30 μg in 15 μL) suspended in 4× sample buffer was loaded into NuPAGE 4% to 12% Bis-Tris Gels (Invitrogen) and transferred to a polyvinyl difluoride membrane. Polyvinyl difluoride membranes were first incubated with primary Ab to p-p65 (Ser 536; Cell Signaling Technology Inc., Danvers, MA), total p65 (Cell Signaling Technology Inc.), or total Rac1 (Transduction Laboratories, Franklin Lakes, NJ) overnight at 4°C by gently rocking and then incubated for 1 hour with the secondary Ab at room temperature. Densitometry analysis was performed on exposed films using the software UN-SCAN-IT version 6.1 (Silk Scientific, Orem, UT).

RNA Isolation and Quantitative PCR Analysis

Total RNA of RPE/choroidal tissues was extracted by TRI Reagent (Sigma-Aldrich). RNA was quantified using a NanoDrop spectrophotometer (Thermo Fisher Scientific,
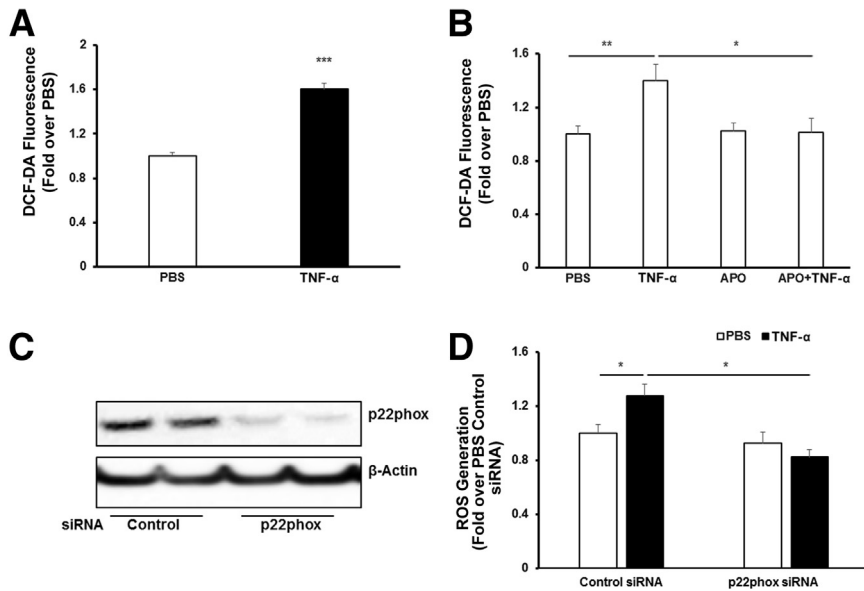
Figure 2 Tumor necrosis factor (TNF)-α induces NADPH oxidase—dependent reactive oxygen species (ROS) generation in choroidal endothelial cells (CECs). ROS generation measured by 2′,7′-dichlorofluorescein (DCF)—diacetate (DA) fluorescence in CECs treated with 20 ng/mL phosphate-buffered saline (PBS) or recombinant human TNF-α for 15 minutes (**A**) and in CECs pre-treated with 100 μmol/L apocynin (APO) for 30 minutes, followed by 15-minute incubation with TNF-α (**B**). Western blots of p22phox (**C**) and ROS generation in CECs by DCF-DA fluorescence transfected with p22phox siRNA or control siRNA and treated with TNF-α or PBS for 15 minutes (**D**). *$P < 0.05$, **$P < 0.01$, and ***$P < 0.001$. $n = 6$.

Waltham, MA). cDNA was generated with the use of a high-capacity cDNA archive kit (Life Technologies, Grand Island, NY). Quantitative PCR was performed on a Mastercycler ep *realplex* system (Eppendorf, Hauppauge, NY) with the use of SYBR Green master mix (Roche Diagnostics, Indianapolis, IN) and primers synthesized by the core research facility of the University of Utah. Expression levels for TNF-α were normalized to the mean value of internal control glyceraldehyde-3-phosphate dehydrogenase. The primers (forward and reverse, respectively) were as follows: mouse TNF-α, 5′-TTGTCTACTCCCAGGTT-CTCT-3′ and 5′-GAGGTTGACTTTCTCCTAATATG-3′; and mouse glyceraldehyde-3-phosphate dehydrogenase,

5′-GGAGAAACCTGCCAAGTATGA-3′ and 5′-TCCTCA-GTGTAGCCCAAGA-3′.

Statistical Analysis

Significant differences between groups were determined by analysis of variance with a post hoc protected Bonferroni multiple comparison test. For animal studies, at least 20 laser spots were analyzed for CNV and 10 retinal sections for DHE. Western blot or PCR analyses included six to eight retinas per condition. For analysis of densitometry of immunolabeled retinas, at least three sections taken at 60-μm intervals were examined per eye, and a total of three
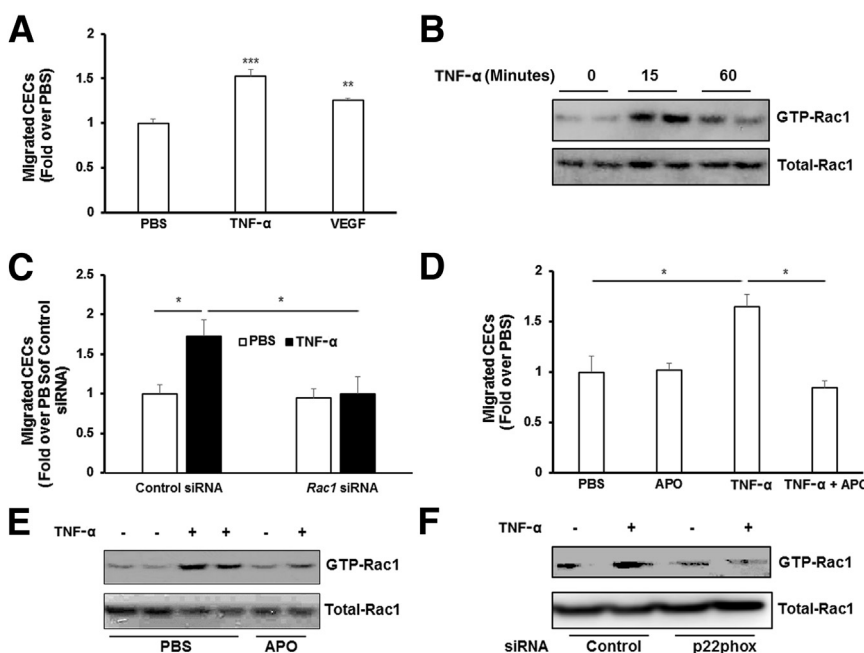

Figure 3 Tumor necrosis factor (TNF)-α induces choroidal endothelial cell (CEC) migration via reactive oxygen species—dependent Rac1 activation. CECs migrating toward 20 ng/mL TNF-α or 20 ng/mL vascular endothelial growth factor (VEGF) were measured after incubation with phosphate-buffered saline (PBS; **A**) or 100 μmol/L apocynin (APO; **D**) . Rac1 activity was analyzed in CECs treated with TNF-α for 0, 15, or 60 minutes (**B**), or pretreated with APO or PBS, followed by 15-minute incubation with TNF-α (**E**) and in CECs transfected with p22phox siRNA or control siRNA and treated with TNF-α or PBS for 15 minutes (**F**). *$P < 0.05$, **$P < 0.01$, and ***$P < 0.001$. $n = 6$ (**C**).
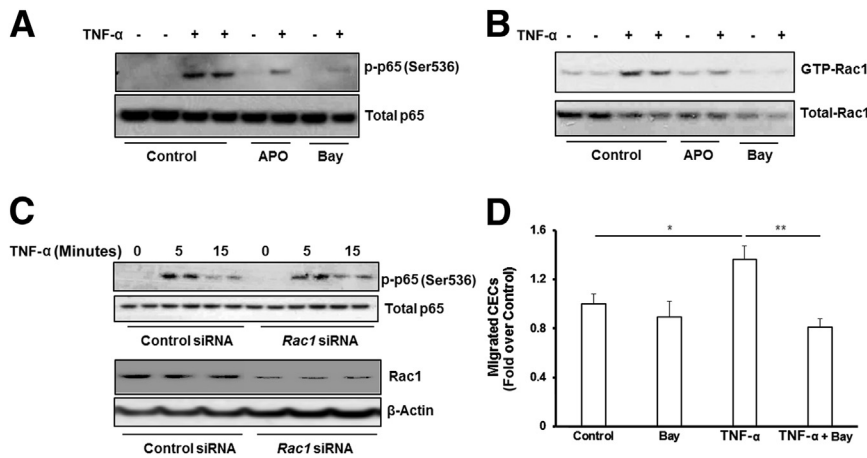
Figure 4 Tumor necrosis factor (TNF)-α induces choroidal endothelial cell (CEC) migration via reactive oxygen species—mediated NF-κB—dependent Rac1 activation. Western blots of p-p65 and total p65 (**A**) and Rac1 activity assay (**B**) were measured in CECs pretreated with 100 μmol/L apocynin (APO) or 1 μmol/L Bay 11-7082 (Bay) for 30 minutes, followed by 15-minute incubation with 20 ng/mL TNF-α or phosphate-buffered saline. **C:** Western blots of p-p65 and total p65, Rac1, and β-actin in CECs transfected with siRNA targeting human *Rac1* gene or control siRNA. **D:** Migrated CECs toward TNF-α or PBS were measured in CECs incubated with Bay 11-7082 or dimethyl sulfoxide. *$P < 0.05$, **$P < 0.01$. $n = 6$.

eyes were used for each condition. For *in vitro* studies, each experimental condition included an $n = 6$ to 9, and each experiment was performed three times. Results were calculated as means ± SEM. $P < 0.05$ was considered statistically significant.

Results

Up-Regulation of TNF-α Is Associated with the Development of CNV in a Murine Model of Laser-Induced CNV

The TNF-α mRNA level in RPE/choroids of mice was significantly increased 5 days after laser injury compared with unlasered mice (Figure 1A). Compared with unlasered controls, TNF-α staining was greater in the overlying retina of laser-treated eyes and also colocalized with isolectin-labeled CECs within CNV (Figure 1B). Similar to previous reports,[7,8] laser-induced CNV volume was significantly reduced in mice treated with intravitreal neutralizing Ab to mouse TNF-α (TNF-α Ab) compared with mice treated with intravitreal isotype IgG control (Figure 1, C and D).

TNF-α Induces ROS Generation around CNV Lesions and in Cultured CECs by Activating NADPH Oxidase

Oxidative stress is implicated in neovascular AMD, and quenching ROS in RPE/choroids by apocynin treatment reduced CNV volume in the laser-induced CNV model.[19] We, therefore, measured ROS generation in RPE/choroids around CNV lesions by quantifying DHE fluorescence and found that in mice treated with intravitreal TNF-α Ab, DHE fluorescence density was significantly decreased compared with that in RPE/choroids from mice treated with control intravitreal IgG (Figure 1, E and F). These results suggest that TNF-α−mediated CNV involved generation of ROS.

To study mechanisms of TNF-α−induced ROS generation, we measured DCF fluorescence in cultured CECs treated with TNF-α or PBS control. Compared with PBS, TNF-α significantly increased DCF fluorescence

(Figure 2A), and this was inhibited in CECs pretreated with apocynin before stimulation with TNF-α (Figure 2B). To determine whether TNF-α−induced ROS generation involved NADPH oxidase activation, CECs were transfected with siRNA to p22phox (Figure 2C), a subunit of NADPH oxidase, or control siRNA. Compared with control, knockdown of p22phox with siRNA did not affect ROS generation when CECs were treated with PBS, but significantly reduced ROS generation in CECs treated with TNF-α (Figure 2D). These data provide evidence that TNF-α modulated NADPH oxidase—dependent ROS generation in CECs.

TNF-α Induces CEC Migration through NADPH Oxidase—Dependent Rac1 Activation

CEC activation and migration are early steps in the development of CNV. To determine whether TNF-α induced CEC migration, the number of migrated CECs toward TNF-α, compared with VEGF or PBS, was quantified. Compared with PBS, TNF-α induced CEC migration to a similar degree as VEGF (Figure 3A), consistent with previous studies.[23] We previously reported that VEGF induced CEC migration by activating Rac1, which then caused ROS generation through activation of NADPH oxidase.[17] We found in that study that siRNA to *Rac1* inhibited ROS generation induced by VEGF.[17] Therefore, we first determined if activation of Rac1 was involved in TNF-α−induced CEC migration. Rac1 activity assays were performed in CECs treated with TNF-α for 15 or 60 minutes. Active Rac1 (GTP-Rac1) was increased in cells treated with TNF-α, with the greater induction noted 15 minutes after treatment (Figure 3B). Knockdown of Rac1 in CECs by siRNA transfection (Figure 4C) prevented TNF-α−induced CEC migration (Figure 3C). We then sought to determine whether TNF-α−induced CEC migration depended on ROS signaling. CECs were incubated with apocynin to quench intracellular ROS or control PBS. In the presence of apocynin, the number of TNF-α−treated CECs that migrated was significantly reduced compared with control (Figure 3D). Pretreatment with apocynin for 30 minutes also partially inhibited TNF-α−induced Rac1 activation (Figure 3E),
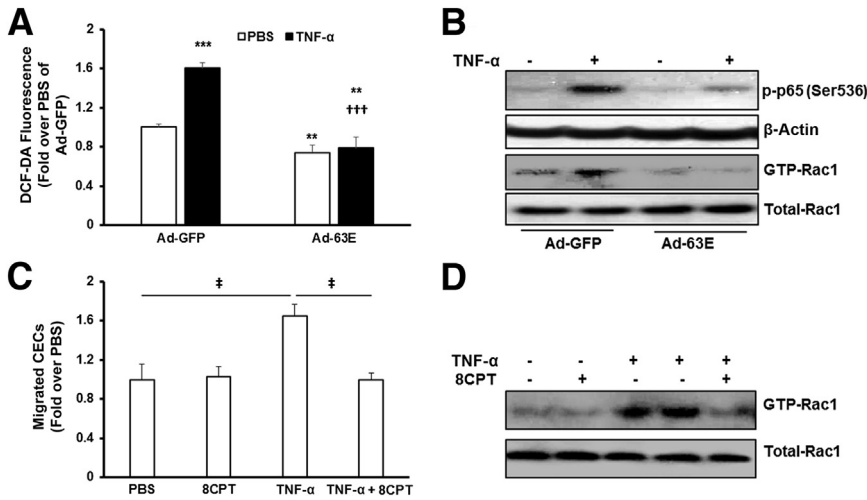
Figure 5 Activation of Rap1 inhibits choroidal endothelial cell (CEC) migration via reactive oxygen species (ROS)—mediated NF-κB and Rac1 activation. ROS generation (**A**), and activation of NF-κB (p-p65) and Rac1 (GTP-Rac1) (**B**) were measured in CECs transduced with adenovirus expressing green fluorescent protein (Ad-GFP) or active Rap1a (Ad-63E) and treated with 20 ng/mL phosphate-buffered saline (PBS) or tumor necrosis factor (TNF)-α for 15 minutes. **C:** Migrated CECs toward TNF-α when CECs were incubated with 50 μmol/L 8-(4-chlorophenylthio)adenosine (8CPT) or PBS. **D:** Rac1 activity assay was measured in CECs pretreated with 8CPT for 30 minutes, followed by 15-minute incubation with TNF-α. **P < 0.01, ***P < 0.001 versus PBS of Ad-GFP; †††P < 0.001 versus tumor necrosis factor (TNF)-α of Ad-GFP; ‡P < 0.05. n = 6 to 9 (**A**); n = 6 (**C**). DCF-DA, 2′,7′-dichlorofluorescein-diacetate.

supporting the thinking that ROS-triggered signaling was upstream of Rac1 activation induced by TNF-α. Compared with control siRNA, knockdown of p22phox inhibited TNF-α—induced Rac1 activation (Figure 3F), additionally supporting the idea that NADPH oxidase—generated ROS also activated Rac1.

Activation of NF-κB Signaling Regulates TNF-α—Mediated Rac1 Activation and CEC Migration

Activation of NF-κB is a classic signaling pathway involved in TNF-α—mediated inflammation. We determined whether activation of NF-κB was involved in TNF-α—mediated CEC migration and Rac1 activation. CECs, pretreated with apocynin or PBS, were stimulated with TNF-α or control, and phospho—NF-κB p65 (p-p65) was measured. NF-κB inhibitor Bay 11-7082 was used as an additional control. The p-p65 increased by TNF-α treatment was partially inhibited by pretreatment with apocynin, but nearly totally inhibited by pretreatment with Bay 11-7082 (Figure 4A). In the same cell lysates, active Rac1 induced by TNF-α was also partially inhibited by apocynin and blocked by pretreatment with Bay 11-7082 (Figure 4B). In CECs transfected with *Rac1* siRNA, TNF-α—induced p-p65 was not decreased compared with control siRNA (Figure 4C), indicating Rac1 activation is the downstream component in this signaling pathway. Furthermore, inhibition of NF-κB by Bay 11-7208 significantly inhibited TNF-α—induced
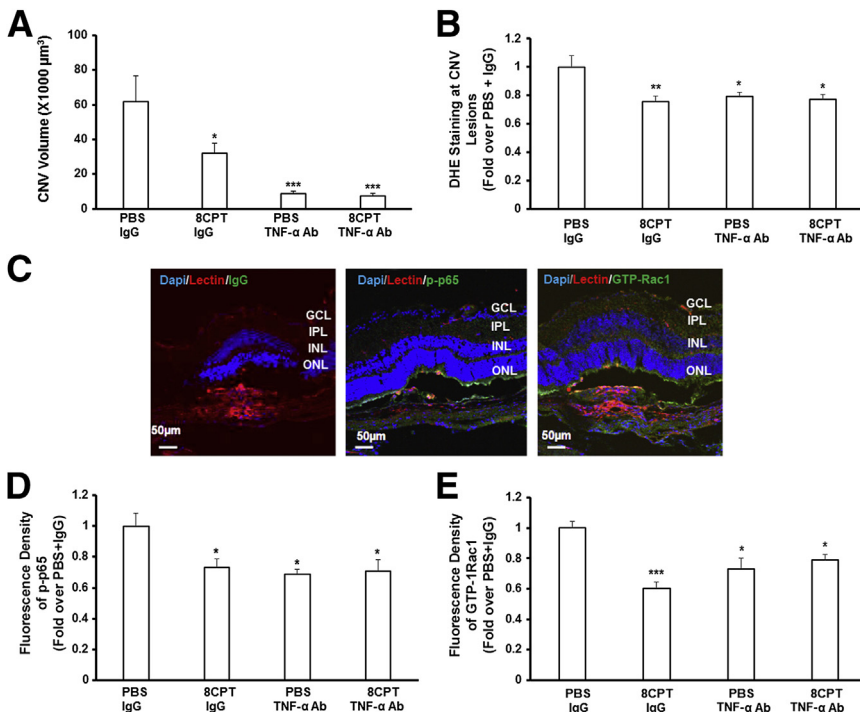

Figure 6 Activation of Rap1 by 8-(4-chlorophenylthio)adenosine (8CPT) reduces choroidal neovascularization (CNV) volume and NF-κB and Rac1 activation in choroidal endothelial cells (ECs) in the laser-induced CNV model. CNV volume (**A**), dihydroethidium (DHE) staining in retinal pigment epithelium (RPE)/choroids (**B**), and immunostaining of p-p65 and GTP-Rac1 (**C**—**E**) in lectin-stained choroidal ECs (CECs) around CNV lesions of mice injected with 0.5 μL phosphate-buffered saline (PBS) + 50 ng IgG, 20.5 μmol/L 8CPT + 50 ng IgG, 50 ng tumor necrosis factor (TNF)-α antibody (Ab) + 0.5 μL PBS, and 20.5 μmol/L 8CPT + 50 ng TNF-α Ab. **C:** Representative images of IgG + PBS treated eyes. **D** and **E:** Densitometry of immunofluorescence of p-p65 and GTP. *P < 0.05, **P < 0.01, and ***P < 0.001 versus PBS + IgG. n = 20 (**A** and **B**); n = 8 (**D** and **E**). GCL, ganglion cell layer; INL, inner nuclear layer; IPL, inner plexiform layer; ONL, outer nuclear layer.
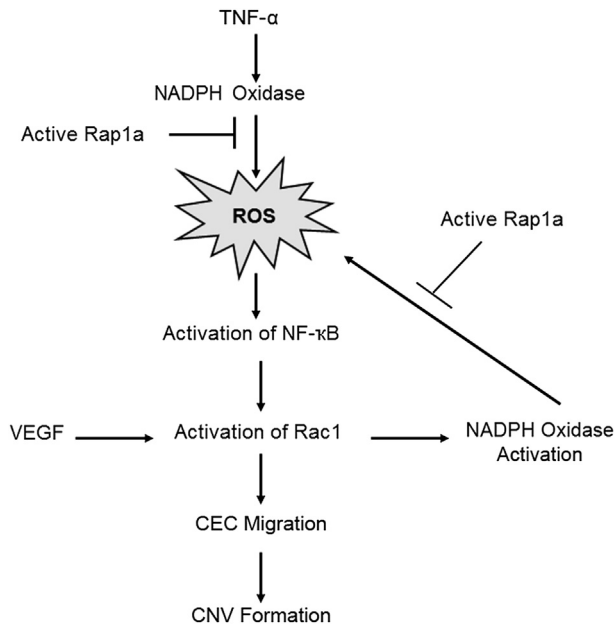
Figure 7 Diagram illustrating the hypothetical signaling pathway and feed-forward loop in inflammation- and oxidative stress−regulated choroidal endothelial cell (CEC) migration and choroidal neovascularization (CNV) formation. ROS, reactive oxygen species; TNF, tumor necrosis factor; VEGF, vascular endothelial growth factor.

CEC migration (Figure 4D). Altogether, these data suggest that intracellular ROS generation by TNF-α, mediating Rac1 activation downstream of NF-κB, ultimately results in decreased CEC migration.

Activation of Rap1 Inhibits TNF-α−Induced CEC Migration and CNV Formation by Inhibiting ROS-Dependent NF-κB and Rac1 Activation

We previously found that expression of active Rap1a, but not active Rap1b, inhibited NADPH oxidase−dependent ROS generation in RPE.[21] Herein, we determined if activated Rap1 could inhibit TNF-α−induced ROS generation in CECs and reduce CEC migration. CECs were incubated with an adenovirus expressing either GFP (Ad-GFP) or active Rap1a (Ad-63E). Forty-eight hours after viral transduction, intracellular ROS generation measured with the DCF-diacetate assay was significantly reduced in CECs transduced with Ad-63E and treated with PBS (Figure 5A), consistent with our published data.[21] Also, in CECs overexpressing active Rap1a and treated with TNF-α, ROS was significantly inhibited compared with CECs treated with TNF-α and control adenovirus, Ad-GFP. In a parallel experiment, TNF-α−induced p-p65 and GTP-Rac1 were also inhibited in CECs transduced with Ad-63E (Figure 5B). These data support the thinking that active Rap1a inhibited ROS, NF-κB, and Rac1. Treatment with Bay 11-7082 did not reduce ROS generation induced by TNF-α treatment (data not shown), providing support that ROS generation was upstream of NF-κB activation. Activation of Rap1 by 8CPT significantly reduced the number of migrating

TNF-α−stimulated CECs compared with control (Figure 5C). 8CPT treatment also inhibited TNF-α−mediated Rac1 activation (Figure 5D). Collectively, our studies provide evidence that activation of Rap1 in CECs inhibited TNF-α−induced CEC migration by reducing ROS-mediated NF-κB−dependent Rac1 activation.

We then tested the hypothesis that Rap1 activation inhibited TNF-α−induced activation of NF-κB and Rac1 in choroidal vessels by reducing ROS *in vivo*. Compared with control intravitreal PBS + IgG, mice in the laser-induced CNV model treated with intravitreal injections of 8CPT + IgG, TNF-α Ab + PBS, or TNF-α Ab + 8CPT had significantly reduced CNV volumes (Figure 6A) and density of DHE fluorescence in RPE/choroids around CNV lesions (Figure 6B). There was no difference in CNV volume or DHE densities in eyes that received intravitreal TNF-α Ab + 8CPT compared with either 8CPT + IgG or TNF-α Ab + PBS injections. Immunostaining of isolectin-stained ECs with p-p65 or GTP-Rac1 (Figure 6C) showed significantly reduced p-p65 (Figure 6D) and GTP-Rac1 (Figure 6E) in RPE/choroids after intravitreal injection of TNF-α Ab or 8CPT, but no additional decrease in p-p65 and GFP-Rac1 in RPE/choroids treated with both 8CPT and TNF-α Ab compared with 8CPT + IgG or TNF-α Ab + PBS. The data shown in Figures 5 and 6 provide evidence that activation of Rap1 with 8CPT inhibits CEC migration and CNV formation mediated through TNF-α−induced ROS and downstream activation of NF-κB−dependent Rac1.

Discussion

Neovascular AMD is a complex disease that involves interactions of several pathways, including those involving inflammation,[9,24] oxidation,[25] hypoxia,[5] aging,[26] and potentially lipid- or cholesterol-related events.[27] Many of these pathways lead to biological processes involving the loss of RPE barrier integrity and the activation of CECs before the development of CNV that causes vision loss in human AMD. Ideally, understanding and addressing the mechanisms of early steps involved in neovascular AMD to prevent compromise of RPE barrier integrity and activation of CECs would be important to prevent vision loss from neovascular AMD. VEGF is involved in early steps involving angiogenesis, but treatments to inhibit VEGF are successful in <50% of patients with neovascular AMD.[2] TNF-α is an inflammatory cytokine that has been reported in the development of CNV in the murine laser−induced CNV model[7] and in human neovascular AMD.[28] However, inhibition of TNF-α with a systemic anti−TNF-α agent infliximab in humans was associated with uveal melanomas, raising possible safety concerns of malignant transformation of benign choroidal nevi.[29] Therefore, we sought to understand the mechanisms involved in these processes.

By using the mouse laser-induced CNV model, we found that laser injury increased TNF-α expression in

RPE/choroids, and that TNF-α colocalized with lectin-stained CECs within the CNV lesion and those migrating toward the CNV. Inhibition of TNF-α bioactivity by intravitreal TNF-α Ab reduced CNV volume in association with decreased ROS in RPE/choroids around CNV lesions. In cultured human CECs, TNF-α induced NADPH oxidase–dependent ROS generation. Intracellular ROS can function as second messengers to activate signaling pathways involved in physiological[30] and pathological[31] processes. In CECs, TNF-α induced CEC migration, and quenching ROS by pretreatment with apocynin significantly inhibited TNF-α–mediated CEC migration. The results in our study support the thinking that TNF-α contributed to CNV formation by mediating ROS-dependent CEC activation and migration.

The Rho GTPase protein Rac1 regulates angiogenesis, cell migration, and invasion.[32] Rac1 activity is controlled by guanine nucleotide exchange factors, which exchange GDP for GTP to activate Rac1, and GTPase-activating proteins, which convert GTP to GDP to inactivate Rac1. Inhibition of Rac1 activity emerges as a therapeutic target in cancer by inhibiting angiogenesis and metastasis. In cultured CECs, we previously showed that VEGF induced CEC migration by activating Rac1, which was upstream of activated NADPH oxidase.[17] Herein, TNF-α–induced CEC migration was also increased via a mechanism involving Rac1 activation. However, TNF-α–induced Rac1 activation appeared downstream of ROS generation in the current study. Our findings suggest a feed-forward loop that augments CEC migration by two pathways involving Rac1 activation through the inflammatory cytokine, TNF-α, and the angiogenic factor, VEGF.

NF-κB activation is implicated in TNF-α–mediated inflammation.[33] A recent study provides evidence that NF-κB activation promotes glioma cell invasion in parallel signaling with Rac1 activation.[34] Therefore, we tested whether activation of NF-κB was involved in TNF-α–mediated CEC migration. Our data showed that TNF-α activated NF-κB in CECs via ROS-dependent signaling. Inhibition of NF-κB by a pharmacological approach inhibited TNF-α–induced CEC migration and Rac1 activation. However, knockdown of Rac1 in CECs did not reduce TNF-α–mediated NF-κB activation, providing evidence that TNF-α–induced activation of NF-κB, mediated by NADPH oxidase, generated ROS upstream of Rac1 activation. These findings suggest additional regulatory mechanisms from those recently reported,[35] in which NF-κB activation during inflammation was found downstream of Rac1.

In cultured RPE, we previously found that activation of Rap1 by pharmacological and genetic approaches inhibited NADPH oxidase–generated ROS by interfering with assembly of NADPH subunits.[21] Herein, we provide evidence that activation of Rap1 through 8CPT can modulate the effects of TNF-α or VEGF on CEC migration and CNV formation through several steps preventing ROS-triggered NF-κB/Rac1 activation.

In summary, we demonstrate evidence that TNF-α–mediated CEC activation and migration occurred by ROS-triggered NF-κB–dependent activation of Rac1 (Figure 7). Preclinical models do not reflect the complexity in neovascular AMD; yet, the models are helpful in assessing outcomes related to injury, inflammation, and oxidation. Our results, along with previous studies, suggest a way in which angiogenic VEGF and inflammatory TNF-α can overwhelm homeostatic mechanisms and thereby allow CNV formation by generating a feed-forward loop. Hypoxia-induced VEGF activates NADPH oxidase through Rac1 to generate intracellular ROS. The inflammatory cytokine TNF-α also acts through NADPH oxidase to generate ROS, which, in turn, through NF-κB, activates Rac1. The biological events after these signaling effects are CEC migration and CNV formation. Thus, Rap1 activation can inhibit CNV induced through VEGF and TNF-α (Figure 7) at several steps.

Acknowledgment

References

1. Joussen AM, Bornfeld N: The treatment of wet age-related macular degeneration. Dtsch Arztebl Int 2009, 106:312−317
2. Ehlken C, Jungmann S, Bohringer D, Agostini HT, Junker B, Pielen A: Switch of anti-VEGF agents is an option for nonresponders in the treatment of AMD. Eye (Lond) 2014, 28:538−545
3. Hartnett ME, Elsner AE: Characteristics of exudative age-related macular degeneration determined in vivo with confocal and indirect infrared imaging. Ophthalmology 1996, 103:58−71
4. Stevens TS, Bressler NM, Maguire MG, Bressler SB, Fine SL, Alexander J, Phillips DA, Margherio RR, Muphy PL, Schachat AP: Occult choroidal neovascularization in age-related macular degeneration: a natural history study. Arch Ophthalmol 1997, 115:345−350
5. Blasiak J, Petrovski G, Vereb Z, Facsko A, Kaarniranta K: Oxidative stress, hypoxia, and autophagy in the neovascular processes of age-related macular degeneration. Biomed Res Int 2014, 2014:768026
6. Sunness JS, Gonzalez-Baron J, Bressler NM, Hawkins B, Applegate CA: The development of choroidal neovascularization in eyes with the geographic atrophy form of age-related macular degeneration. Ophthalmology 1999, 106:910−919
7. Lichtlen P, Lam TT, Nork TM, Streit T, Urech DM: Relative contribution of VEGF and TNF-alpha in the cynomolgus laser-induced CNV model: comparing the efficacy of bevacizumab, adalimumab, and ESBA105. Invest Ophthalmol Vis Sci 2010, 51:4738−4745
8. Jasielska M, Semkova I, Shi X, Schmidt K, Karagiannis D, Kokkinou D, Mackiewicz J, Kociok N, Joussen AM: Differential role of tumor necrosis factor (TNF)-alpha receptors in the development of choroidal neovascularization. Invest Ophthalmol Vis Sci 2010, 51:3874−3883
9. Markomichelakis NN, Theodossiadis PG, Sfikakis PP: Regression of neovascular age-related macular degeneration following infliximab therapy. Am J Ophthalmol 2005, 139:537−540
10. Theodossiadis PG, Liarakos VS, Sfikakis PP, Vergados IA, Theodossiadis GP: Intravitreal administration of the anti-tumor

necrosis factor agent infliximab for neovascular age-related macular degeneration. Am J Ophthalmol 2009, 147:825−830, 830.e1

11. Fuggle NR, Howe FA, Allen RL, Sofat N: New insights into the impact of neuro-inflammation in rheumatoid arthritis. Front Neurosci 2014, 8:357

12. Laveti D, Kumar M, Hemalatha R, Sistla R, Naidu VG, Talla V, Verma V, Kaur N, Nagpal R: Anti-inflammatory treatments for chronic diseases: a review. Inflamm Allergy Drug Targets 2013, 12:349−361

13. Park J, Min JS, Kim B, Chae UB, Yun JW, Choi MS, Kong IK, Chang KT, Lee DS: Mitochondrial ROS govern the LPS-induced pro-inflammatory response in microglia cells by regulating MAPK and NF-kappaB pathways. Neurosci Lett 2015, 584:191−196

14. Li JM, Fan LM, Christie MR, Shah AM: Acute tumor necrosis factor alpha signaling via NADPH oxidase in microvascular endothelial cells: role of p47phox phosphorylation and binding to TRAF4. Mol Cell Biol 2005, 25:2320−2330

15. Peshavariya HM, Taylor CJ, Goh C, Liu GS, Jiang F, Chan EC, Dusting GJ: Annexin peptide Ac2-26 suppresses TNFalpha-induced inflammatory responses via inhibition of Rac1-dependent NADPH oxidase in human endothelial cells. PLoS One 2013, 8:e60790

16. Kofler S, Nickel T, Weis M: Role of cytokines in cardiovascular diseases: a focus on endothelial responses to inflammation. Clin Sci (Lond) 2005, 108:205−213

17. Peterson LJ, Wittchen ES, Geisen P, Burridge K, Hartnett ME: Heterotypic RPE-choroidal endothelial cell contact increases choroidal endothelial cell transmigration via PI 3-kinase and Rac1. Exp Eye Res 2007, 84:737−744

18. Wang H, Geisen P, Wittchen ES, King B, Burridge K, D'Amore PA, Hartnett ME: The role of RPE cell-associated VEGF189 in choroidal endothelial cell transmigration across the RPE. Invest Ophthalmol Vis Sci 2011, 52:570−578

19. Monaghan-Benson E, Hartmann J, Vendrov AE, Budd S, Byfield G, Parker A, Ahmad F, Huang W, Runge M, Burridge K, Madamanchi N, Hartnett ME: The role of vascular endothelial growth factor-induced activation of NADPH oxidase in choroidal endothelial cells and choroidal neovascularization. Am J Pathol 2010, 177:2091−2102

20. Wittchen ES, Nishimura E, McCloskey M, Wang H, Quilliam LA, Chrzanowska-Wodnicka M, Hartnett ME: Rap1 GTPase activation and barrier enhancement in RPE inhibits choroidal neovascularization in vivo. PLoS One 2013, 8:e73070

21. Wang H, Jiang Y, Shi D, Quilliam LA, Chrzanowska-Wodnicka M, Wittchen ES, Li DY, Hartnett ME: Activation of Rap1 inhibits NADPH oxidase-dependent ROS generation in retinal pigment epithelium and reduces choroidal neovascularization. FASEB J 2014, 28:265−274

22. Committee for the Update of the Guide for the Care and Use of Laboratory AnimalsNational Research Council: Guide for the Care and Use of Laboratory Animals: Eighth Edition. Washington, DC, National Academies Press, 2011

23. Wang H, Wittchen ES, Jiang Y, Ambati B, Grossniklaus HE, Hartnett ME: Upregulation of CCR3 by age-related stresses promotes choroidal endothelial cell migration via VEGF-dependent and -independent signaling. Invest Ophthalmol Vis Sci 2011,, 52:8271−8277

24. Despriet DD, Klaver CC, Witteman JC, Bergen AA, Kardys I, de Maat MP, Boekhoorn SS, Vingerling JR, Hofman A, Oostra BA, Uitterlinden AG, Stijnen T, van Duijn CM, de Jong PT: Complement factor H polymorphism, complement activators, and risk of age-related macular degeneration. JAMA 2006, 296:301−309

25. Crabb JW, Miyagi M, Gu X, Shadrach K, West KA, Sakaguchi H, Kamei M, Hasan A, Yan L, Rayborn ME, Salomon RG, Hollyfield JG: Drusen proteome analysis: an approach to the etiology of age-related macular degeneration. Proc Natl Acad Sci U S A 2002, 99: 14682−14687

26. Mullins RF, Russell SR, Anderson DH, Hageman GS: Drusen associated with aging and age-related macular degeneration contain proteins common to extracellular deposits associated with atherosclerosis, elastosis, amyloidosis, and dense deposit disease. FASEB J 2000, 14: 835−846

27. Curcio CA, Presley JB, Malek G, Medeiros NE, Avery DV, Kruth HS: Esterified and unesterified cholesterol in drusen and basal deposits of eyes with age-related maculopathy. Exp Eye Res 2005, 81:731−741

28. Wan L, Lin HJ, Tsai Y, Lee CC, Tsai CH, Tsai FJ, Tsai YY, Lin JM: Tumor necrosis factor-alpha gene polymorphisms in age-related macular degeneration. Retina 2010, 30:1595−1600

29. Damento G, Kavoussi SC, Materin MA, Salomao DR, Quiram PA, Balasubramaniam S, Pulido JS: Clinical and histologic findings in patients with uveal melanomas after taking tumor necrosis factor-alpha inhibitors. Mayo Clin Proc 2014, 89:1481−1486

30. Droge W: Free radicals in the physiological control of cell function. Physiol Rev 2002, 82:47−95

31. Weinberg F, Hamanaka R, Wheaton WW, Weinberg S, Joseph J, Lopez M, Kalyanaraman B, Mutlu GM, Budinger GR, Chandel NS: Mitochondrial metabolism and ROS generation are essential for Kras-mediated tumorigenicity. Proc Natl Acad Sci U S A 2010, 107: 8788−8793

32. Bid HK, Roberts RD, Manchanda PK, Houghton PJ: RAC1: an emerging therapeutic option for targeting cancer angiogenesis and metastasis. Mol Cancer Ther 2013, 12:1925−1934

33. Van Antwerp DJ, Martin SJ, Kafri T, Green DR, Verma IM: Suppression of TNF-alpha-induced apoptosis by NF-kappaB. Science 1996, 274:787−789

34. Tran NL, McDonough WS, Savitch BA, Fortin SP, Winkles JA, Symons M, Nakada M, Cunliffe HE, Hostetter G, Hoelzinger DB, Rennert JL, Michaelson JS, Burkly LC, Lipinski CA, Loftus JC, Mariani L, Berens ME: Increased fibroblast growth factor-inducible 14 expression levels promote glioma cell invasion via Rac1 and nuclear factor-kappaB and correlate with poor patient outcome. Cancer Res 2006, 66:9535−9542

35. Cuadrado A, Martin-Moldes Z, Ye J, Lastres-Becker I: Transcription factors NRF2 and NF-kappaB are coordinated effectors of the Rho family, GTP-binding protein RAC1 during inflammation. J Biol Chem 2014, 289:15244−15258